Using Feature Flow Fields for Topological Comparison of Vector Fields

Holger Theisel Christian Rössl Hans-Peter Seidel

Max-Planck-Institut für Informatik, Stuhlsatzenhausweg 85, 66123 Saarbrücken, Germany
Email: {theisel,roessl,hpseidel}@mpi-sb.mpg.de

Abstract

In this paper we propose a new topology based metric for 2D vector fields. This metric is based on the concept of feature flow fields. We show that it incorporates both the characteristics and the local distribution of the critical points while keeping the computing time reasonably small even for topologically complex vector fields. Finally, we apply the metric to track the topological behavior in a time-dependent vector field, and to evaluate a smoothing procedure on a noisy steady vector field.

1 Introduction

Vector fields describing the flow of certain materials belong to the most common data sets which are considered in scientific visualization. To deal with the increasing size and complexity of the vector fields to be visualized, a number of reconstruction, compression and simplification techniques have been introduced. All these techniques rely on certain distance measures between vector fields: the original and the derived vector field have to be compared to guarantee a sufficient similarity between them. Hence the definition of useful metrics on vector fields plays a crucial role in the applications above.

The first approaches on metrics (distance measures) of vector fields consider local deviations of direction and magnitude of the flow vectors in a certain number of sample points ([5], [12]). These distance functions give a fast comparison of the vector field but do not take any structural information of the vector fields into consideration.

One of the most important features of vector fields are their topological skeletons. After their introduction as a visualization tool in [6], a number of extensions have been proposed ([11, 19, 3, 21]) Topological methods are used to simplify [3, 4, 17, 18], smooth [20], compress [8, 14] and design [13] vector fields.

Due to the importance of vector field topology, it is an obvious approach to define vector field metrics which are based on a comparison of the topological skeleton. The topological skeleton of a vector field essentially consists of critical points and separatrices. Given a 2D vector field

$$\mathbf{v}(x,y) = \begin{pmatrix} u(x,y) \\ v(x,y) \end{pmatrix},$$

a first order critical point in $\mathbf{v}$ is an isolated point (x_0, y_0) with $\mathbf{v}(x_0, y_0) = (0,0)^T$ and $\det(\mathbf{J}_\mathbf{v}(x_0, y_0)) \neq 0$, where

$$\mathbf{J}_\mathbf{v}(x,y) = \begin{pmatrix} u_x(x,y) & u_y(x,y) \\ v_x(x,y) & v_y(x,y) \end{pmatrix}$$

denotes the Jacobian matrix field. Separatrices are stream lines which separate the flow into regions of different flow behavior.

A first approach to define a topology based distance function for vector fields was given in [7]. The algorithm described there follows the following scheme:

Algorithm 1 *(find the distance* dist *of the vector fields $\mathbf{v}_1$ and $\mathbf{v}_2$ over the same domain)*

1. *Extract all critical points of $\mathbf{v}_1$ and $\mathbf{v}_2$ and give them a qualitative characterization.*
2. *Couple the critical points in $\mathbf{v}_1$ and $\mathbf{v}_2$: for each critical point in $\mathbf{v}_1$, a partner critical point in $\mathbf{v}_2$ is searched and vice versa. If the number of critical points in $\mathbf{v}_1$ and $\mathbf{v}_2$ does not coincide, additional critical points are introduced.*
3. *Compute the distance of $\mathbf{v}_1$ and $\mathbf{v}_2$ as the summation of the distances of the corresponding critical points.*

Note that algorithm 1 reduces the problem of comparing vector fields to the problem of comparing critical points. To carry out this algorithm, two problems have to be solved:

- A distance function between two critical points has to be introduced.
- A coupling strategy of the critical points of $\mathbf{v}_1$ and $\mathbf{v}_2$ has to be found.

For both problems, a number of solutions have been proposed. It is the main contribution of this paper to introduce a new coupling strategy for the critical points of two vector fields. This strategy is based on the concept of feature flow fields ([15]).

The rest of the paper is organized as follows: section 2 reviews previous work on topology based vector field metrics. Section 3 introduces the concept of feature flow fields. Based on this, section 4 describes how to apply them to couple critical points. Section 5 shows some results, while conclusions are drawn in section 6.

2 Previous Work

Following the outline of algorithm 1, we review both methods to compare critical points and to couple them.

2.1 Distance functions for critical points

To compare two first order critical points, a distance function on their Jacobian matrices has to be introduced. In [7], a critical point is mapped onto the rim of a unit circle in an (α, β) phase plane by

$$p = \text{div}(\mathbf{v}) = u_x + v_y \quad , \quad q = \det(\mathbf{J_v})$$
$$\hat{\alpha} = p \quad , \quad \hat{\beta} = \text{sign}(p^2 - 4q) \cdot \sqrt{\|(p^2 - 4q\|}$$
$$\alpha = \frac{\hat{\alpha}}{\sqrt{\hat{\alpha}^2 + \hat{\beta}^2}} \quad , \quad \beta = \frac{\hat{\beta}}{\sqrt{\hat{\alpha}^2 + \hat{\beta}^2}}.$$

To compare two critical points, their Euclidian distance in the (α, β) phase plane are considered. This (α, β) location reflects important structural similarities of critical points. For instance, the distance of two saddle points in the (α, β) phase plane is less or equal $\sqrt{2}$, while two centers always have identical (α, β) values. However, some structural properties could not be covered by the (α, β) phase plane, such as the collapsing of critical points with different flow behavior or an inconsistent treatment of inverted vector fields (see [16]).

In [16], a (γ, r) phase plane was introduced which maps a critical point into the inner of a unit circle: a critical point gets the polar coordinates (γ, r) as

$$\cos\gamma = \frac{u_x + v_y}{\sqrt{(u_x + v_y)^2 + (v_x - u_y)^2}}$$
$$\sin\gamma = \frac{v_x - u_y}{\sqrt{(u_x + v_y)^2 + (v_x - u_y)^2}}$$
$$r = \frac{1}{2} + \frac{u_x\, v_y - v_x\, u_y}{u_x^2 + v_x^2 + u_y^2 + v_y^2}$$

where u_x, v_x, u_y, v_y denote the components of the Jacobian matrix $\mathbf{J_v}$ at the critical point. See [16] for a discussion of the properties of the (γ, r) phase plane. Similar to the (α, β) phase plane, the distance of two critical points is denoted by the Euclidian distance in the (γ, r) plane.

2.2 Coupling strategies for critical points

Obviously, the coupling strategy for critical points greatly influences the vector field metric. In [7], all possible couplings of the critical points of two vector fields $\mathbf{v}_1$ and $\mathbf{v}_2$ are considered, and the coupling with a minimal summation of the distances of the critical point couples (using the distance in (α, β) space) is searched. To find this optimal coupling, a technique from image retrieval called Earth Mover's Distance (EMD, see [10]) was applied. However, this techniques has a limited applicability due to the following disadvantages:

- The EMD strategy of [7] considers only the characteristics of of critical points, not their location in the vector field. Thus, the distribution of the critical points does not influence the metric.
- Since in worst case all possible couplings of critical points have to be checked, the worst case complexity of the algorithm is $O(n!)$. However, [9] states that in reality the complexity of the algorithm is $O(n^3)$ where n is the number of critical points.

The first problem has partially been resolved in [2] by considering not only the critical points but also their connectivity by separatrices. Since in general there seem to be certain correlations between the connectivity and the location of the critical points, location information is partially considered in [2]. However, the second problem remains unsolved, especially when vector fields of a complex topology (i.e., with a high number of critical points) are treated. In these cases, even a cubic complexity may

drop the computing time to unacceptable rates. In fact, all the examples in [7] (and the follow-up papers [2] and [1]) consider only vector fields with a very small number of critical points.

To overcome the problems mentioned above, we propose a new coupling strategy which is based the recently introduced concept of feature flow fields. In the next section we give a brief introduction to feature flow fields.

3 Feature Flow Fields

Feature flow fields ([15]) originally have been introduced to track features – in particular critical points – in time-dependent vector fields. Given a 2D time-dependent vector field

$$\mathbf{w}(x,y,t) = \begin{pmatrix} u(x,y,t) \\ v(x,y,t) \end{pmatrix}, \qquad (1)$$

a 3D vector field

$$\mathbf{f}(x,y,t) = \begin{pmatrix} f(x,y,t) \\ g(x,y,t) \\ h(x,y,t) \end{pmatrix} \qquad (2)$$

is constructed in such a way that the paths of the critical points over time correspond to stream lines of $\mathbf{f}$. The vector field $\mathbf{f}$ is called feature flow field because its stream lines describe the flow of the features in $\mathbf{v}$. This way the process of tracking a feature is carried out by a numerical stream line integration of $\mathbf{f}$ which is a well-understood procedure in the visualization community. Figure 1 gives an illustration of the concept of feature flow fields.

The particular definition of $\mathbf{f}$ depends on the choice of the feature to be tracked. For our application, we want to track the location of critical points over time. To do so, $\mathbf{f}$ can be written as (see [15])

$$\mathbf{f}(x,y,t) = \begin{pmatrix} \det(\mathbf{w}_y, \mathbf{w}_t) \\ \det(\mathbf{w}_t, \mathbf{w}_x) \\ \det(\mathbf{w}_x, \mathbf{w}_y) \end{pmatrix} \qquad (3)$$

where $\mathbf{w}_x, \mathbf{w}_y, \mathbf{w}_t$ denote the partial derivatives of $\mathbf{w}(x,y,t)$.

4 Applying Feature Flow Fields for Coupling Critical Point

Given are two vector fields $\mathbf{v}_1$ and $\mathbf{v}_2$ over the same domain. To couple the critical points of $\mathbf{v}_1$ and $\mathbf{v}_2$,

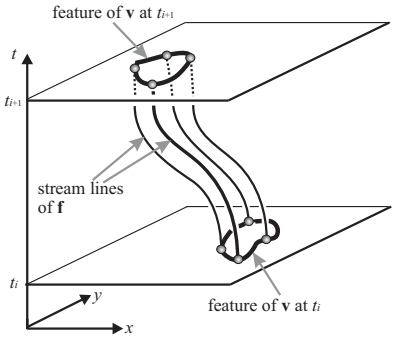

Figure 1: Feature tracking using feature flow fields. The dynamic behavior of a feature of $\mathbf{v}$ at a certain time t_i is tracked by tracing the stream lines of $\mathbf{f}$ from the feature. The features at a certain time t_{i+1} can be observed by intersecting these stream lines with the time plane $t = t_{i+1}$.

we construct a time-dependent vector field $\mathbf{w}$ by applying a linear interpolation of $\mathbf{v}_1$ and $\mathbf{v}_2$:

$$\mathbf{w}(x,y,t) \;=\; (1-t)\;\mathbf{v}_1(x,y) + t\;\mathbf{v}_2(x,y). \qquad (4)$$

Then the feature flow field $\mathbf{f}$ is computed by applying (3) to (4). For every critical point (x_0, y_0) of $\mathbf{v}_1$, the stream line of $\mathbf{f}$ starting from $(x_0, y_0, 0)$ is integrated until one of the following events occur for the current point (x_n, y_n, t_n) of the numerical integration:

1. $t_n \leq 0$: the end point (x_n, y_n) is a critical point in $\mathbf{v}_1$
2. $t_n \geq 1$: the end point (x_n, y_n) is a critical point in $\mathbf{v}_2$
3. (x_n, y_n) lies outside the domain of $\mathbf{v}_1$ and $\mathbf{v}_2$

Figure 2 gives an illustration of the three possible cases.

In case 1 and 3, no partner point of (x_0, y_0) is detected. If case 2 occurs, it can be shown (see [15]) that (x_n, y_n) is a critical point in $\mathbf{v}_2$. In this case, (x_0, y_0) in $\mathbf{v}_1$ and (x_n, y_n) in $\mathbf{v}_2$ are considered to be a couple. A similar approach can be applied to find a partner critical point for $(x_0, y_0, 1)$ in $\mathbf{v}_2$.

Now we can describe the modification of algorithm 1 by using feature flow fields as

Algorithm 2 *(find the topological distance* dist *of the vector fields* $\mathbf{v}_1$ *and* $\mathbf{v}_2$ *over the same domain)*

1. *Extract all critical points of* $\mathbf{v}_1$ *and* $\mathbf{v}_2$.
2. *Construct* $\mathbf{w}$ *and* $\mathbf{f}$ *according to (3) and (4).*

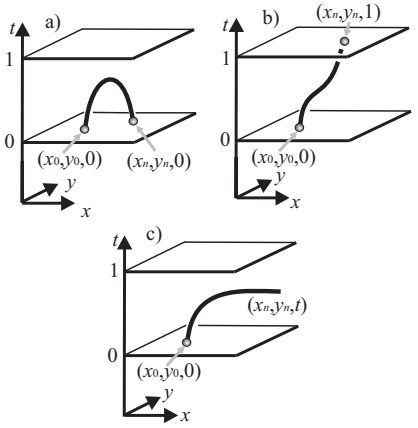

Figure 2: Computing the streamlines of $\mathbf{f}$ starting from a critical point $(x_0, y_0, 0)$ in $\mathbf{v}_1$; a) integration ends in a critical point $(x_n, y_n, 0)$ in $\mathbf{v}_1$; a) integration ends in a critical point $(x_n, y_n, 1)$ in $\mathbf{v}_2$; c) integration leaves the domain of $\mathbf{v}_1$ and $\mathbf{v}_2$.

3. *for every critical point (x_0, y_0) of $\mathbf{v}_1$: integrate the stream line of $\mathbf{f}$ starting in $(x_0, y_0, 0)$. If the integration ends in a point $(x_n, y_n, 1)$, the critical point (x_n, y_n) in $\mathbf{v}_2$ is the partner of (x_0, y_0) in $\mathbf{v}_1$. Otherwise, no partner critical point of (x_0, y_0) is detected.*
4. *Detect partner points for all critical points of $\mathbf{v}_2$ which do not have a partner yet, by applying an approach similar to 3.*
5. *Compute the distance* dist *of $\mathbf{v}_1$ and $\mathbf{v}_2$ as the summation of the Euclidian distances of the corresponding critical points in (γ, r) phase plane. If a critical point does not have a partner, its contribution to the summation is set to 2 (the maximal distance in (γ, r) phase plane).*

Before applying algorithm 2, we have to ensure that it really defines a metric on all vector fields over the same domain:

Theorem 1 *The distance function* dist *defined by algorithm 2 is a metric on the set of all vector fields over the same domain.*

Proof:

1. $\text{dist}(\mathbf{v}_1, \mathbf{v}_1) = 0$: inserting $\mathbf{v}_1 = \mathbf{v}_2$ into (3) and (4) gives $\mathbf{f}(x, y, t) = (0, 0, h(x, y, t))^T$. Thus, every critical point of $\mathbf{v}_1$ is mapped to itself contributing a zero distance to the dist function. Figure 3 gives an illustration using a data set which is explained later in section 5.
2. $\text{dist}(\mathbf{v}_1, \mathbf{v}_2) = \text{dist}(\mathbf{v}_2, \mathbf{v}_1)$ follows directly from the symmetry of the linear interpolation in (4).
3. $\text{dist}(\mathbf{v}_1, \mathbf{v}_3) \leq \text{dist}(\mathbf{v}_1, \mathbf{v}_2) + \text{dist}(\mathbf{v}_2, \mathbf{v}_3)$: Let (x_0, y_0) be a critical point in $\mathbf{v}_1$. If (x_0, y_0) as partner critical point (x_n, y_n) in $\mathbf{v}_2$, we compute the partner of (x_n, y_n) in $\mathbf{v}_3$ by $\text{dist}(\mathbf{v}_2, \mathbf{v}_3)$. If this partner in $\mathbf{v}_3$ exists, we call it (x_m, y_m). If one of the points (x_n, y_n) or (x_m, y_m) does not exist, the inequality is fulfilled because one of the summands on the right-hand side has the maximal value of 2. If both (x_n, y_n) or (x_m, y_m) exist, the inequality is fulfilled because the Euclidian distance of (x_0, y_0), (x_n, y_n), (x_m, y_m) in the (γ, r) plane is a metric.

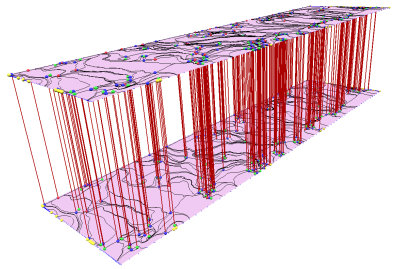

Figure 3: Comparing the vector field with itself: $\mathbf{f}$ maps every critical point to itself.

5 Results

We show the application of our distant measure for two problems: the comparison of different time steps in a time varying data set, and the evaluation of a smoothing procedure in a noisy flow data set.

Give a time-dependent vector field, one of the most crucial tasks is to explore the temporal behavior of its important feature. Figure 4 shows the visualization of a 2D flow in a bay area of the Baltic Sea near Greifswald, Germany (Greifswalder Bodden) at three different time steps. This data set was obtained by a numerical simulation on a regular 115×103 grid at 25 time steps. It was created by the Department of Mathematics, University of Rostock (Germany). The data set can be considered as a collection of 25 vector fields $\mathbf{v}_0, ..., \mathbf{v}_{24}$.

Figure 4 shows the topological skeleton of the first and the last vector field $\mathbf{v}_0$ and $\mathbf{v}_{24}$ as well as the vector field $\mathbf{v}_{11}$ approximately in the middle of the time sequence. To evaluate the temporal behavior of

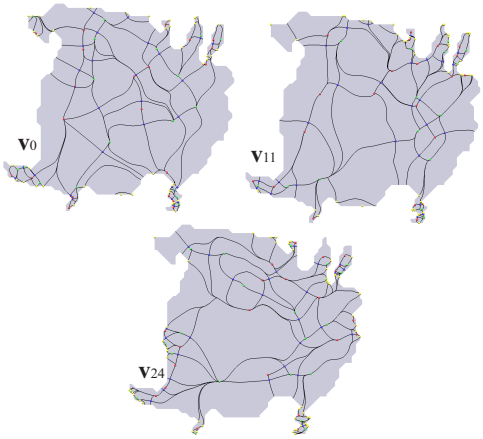

Figure 4: Topological skeleton of the bay data set at the time steps 0, 11 and 24.

the topology, we computed the topological distance of each time step with all other time steps, i.e. we compute dist$(\mathbf{v}_i, \mathbf{v}_j)$ for all $i, j \in \{0, ..., 24\}$. As an example, figure 5 illustrates the computation of the distance of the vector fields $\mathbf{v}_5$ and $\mathbf{v}_{10}$. Shown are the topological skeletons of $\mathbf{v}_5$ and $\mathbf{v}_{10}$ as well as the integration of the stream lines of the feature flow field starting in the critical point. We can see that most of the points find their partners in the other vector field. Figure 6 shows a magnification of figure 5).

Figure 7 shows the color coded distance matrix of all vector fields $\mathbf{v}_0, ..., \mathbf{v}_{24}$. The distance varied between 0 and a maximal value of 104.5 (which was detected between $\mathbf{v}_3$ and $\mathbf{v}_{24}$). We linearly color coded the distance in such a way that a zero distance corresponds to black while the maximal distance corresponds to white. Figure 7 shows that the distance matrix is symmetric and with a zero main diagonal. This corresponds to the observation that our distant measure is a metric. The most important observation which can be made from figure 7 is that the distance of two vector fields $\mathbf{v}_i$ and $\mathbf{v}_j$ is approximately proportional to the distance $\|i - j\|$ of the time indices. This means that the rate of change of the topology is approximately linear

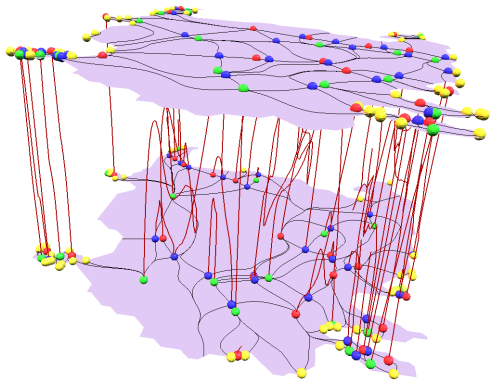

Figure 5: Coupling the critical points of the $\mathbf{v}_5$ and $\mathbf{v}_{10}$ of the bay data set by integrating the stream lines of $\mathbf{f}$.

over time. This result is particularly interesting if we consider the number of critical points in the vector fields $\mathbf{v}_0, ..., \mathbf{v}_{24}$. They are (in this order) 65, 71, 71, 68, 65, 71, 63, 62, 66, 64, 65, 63, 70, 70, 51, 61, 52, 50, 56, 52, 63, 62, 72, 65. This shows that there is no correlation between the number of critical points and the topological distance: both $\mathbf{v}_0$ and $\mathbf{v}_{24}$ have the same number 65 of critical points but a maximal topological distance.

Figure 8 shows the topological skeleton of a vector field $\mathbf{v}_0$ describing the skin friction on a face of a cylinder which was obtained by a numerical simulation of a flow around a square cylinder. The data set was generated by R.W.C.P. Verstappen and A.E.P. Veldman of the University of Groningen (the Netherlands). The data was given on a rectangular 102 x 64 grid with varying grid size and consists of 338 critical points, 34 boundary switch points, and 714 separatrices. Therefore, it can be considered as a vector field of a complex topology. From this vector field $\mathbf{v}_0$ we created a number of new vector fields $\mathbf{v}_i$ $(i = 0, ..., 30)$ by applying i iterations of a Laplacian smoothing of $\mathbf{v}_0$. We compute the topological distance of all $\mathbf{v}_i$ in order to get an assessment of the smoothing.

Figure 9 shows the stream lines of the feature flow field between $\mathbf{v}_0$ and $\mathbf{v}_{10}$. As we can see there, most of the critical points of $\mathbf{v}_0$ do not have partner in $\mathbf{v}_{10}$. Figure 10 shows a magnification of figure 9. Figure 11 illustrates the coupling process between the critical points of $\mathbf{v}_0$ and $\mathbf{v}_{30}$

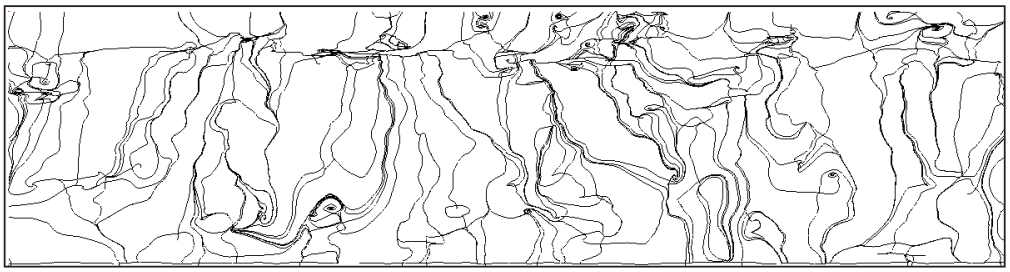

Figure 8: Topological skeleton of the original skin friction data set.

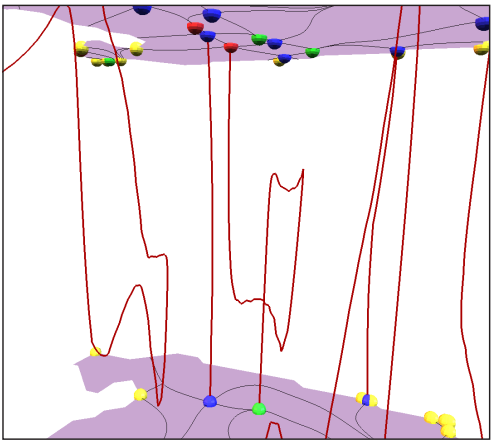

Figure 6: Coupling the critical points of the $\mathbf{v}_5$ and $\mathbf{v}_{10}$ (magnification of figure 5).

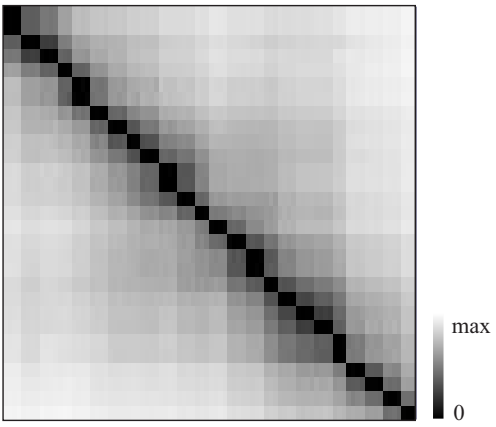

Figure 7: Distance matrix between $\mathbf{v}_0$,...,$\mathbf{v}_{24}$ for the bay data set.

Figure 12 shows the distance matrix of all vector fields $\mathbf{v}_0, ...\mathbf{v}_{30}$ of the skin friction data set. The distance varied between 0 and 336.15 (between $\mathbf{v}_0$ and $\mathbf{v}_{22}$). As we can see in the picture, there is a significant distance between $\mathbf{v}_0$ and all the other vector fields. The remaining distances between $\mathbf{v}_i$ and $\mathbf{v}_j$ $(i, j \neq 0)$ are approximately proportional to $\|i - j\|$.

The interpretation of the distance matrix in figure 12 is that the original data set consists of a lot of noise which was almost entirely smoothed out by applying a Laplacian smoothing once. Further smoothing had only a little influence on the topology of the data set.

The time to compute dist$(\mathbf{v}_i, \mathbf{v}_j)$ strongly depends on the number of critical points of $\mathbf{v}_i$ and $\mathbf{v}_j$. It was less than 10 seconds for any pair $i, j \in \{0, ..., 30\}$ on an Intel Xeon 1.7 GHz processor.

6 Conclusions

We have introduced a new distance measure for 2D vector fields which is based on the concept of feature flow fields. This distance measure has been shown to be fast and reliable even for topologically complex data sets. It yields a natural approach of coupling critical points of two vector fields in such a way that both the characteristics and the location of the critical points are considered. We applied the measure to two real-life data sets to evaluate the temporal evolving of a time-dependent flow data set and the smoothing of a noisy steady flow data set.

For future research, we intend to apply a similar distance measure to 3D vector fields.

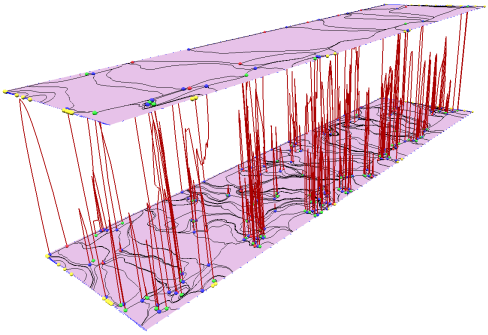

Figure 9: Coupling the critical points of the $\mathbf{v}_0$ and $\mathbf{v}_{10}$ (skin friction data set).

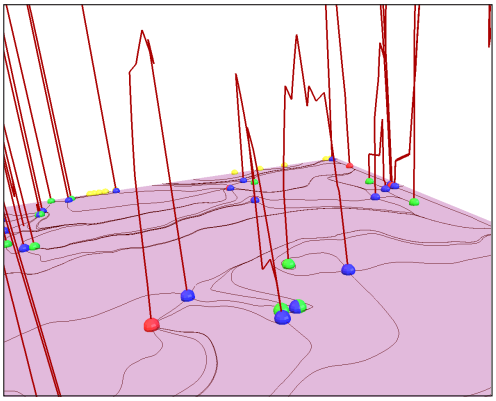

Figure 10: Magnification of figure 9.

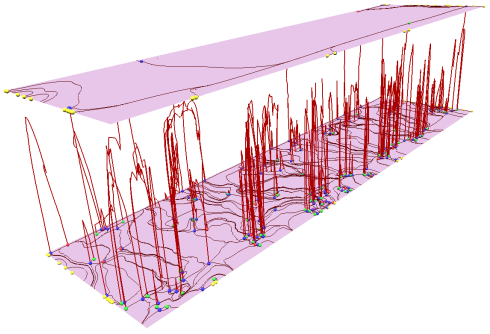

Figure 11: Coupling the critical points of the $\mathbf{v}_0$ and $\mathbf{v}_{30}$ (skin friction data set).

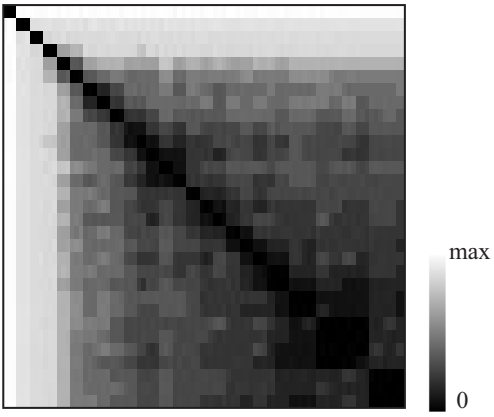

Figure 12: Distance matrix of $\mathbf{v}_0, ..., \mathbf{v}_{30}$ (skin friction data set).

Acknowledgements

The authors thank Wim de Leeuw for providing the skin friction data set.

References

[1] R. Batra and L. Hesselink. Feature comparisons of 3-D vector fields using earth mover's distance. In *Proc. IEEE Visualization '99*, pages 105–114, 1999.

[2] R. Batra, K. Kling, and L. Hesselink. Topology based vector field comparison using graph methods. In *Proc. IEEE Visualization '99, Late Breaking Hot Topics*, pages 25–28, 1999.

[3] W. de Leeuw and R. van Liere. Collapsing flow topology using area metrics. In D. Ebert, M. Gross, and B. Hamann, editors, *Proc. IEEE Visualization '99*, pages 149–354, Los Alamitos, 1999.

[4] W. de Leeuw and R. van Liere. Visualization of global flow structures using multiple levels of topology. In *Data Visualization 1999. Proc. VisSym 99*, pages 45–52, 1999.

[5] B. Heckel, G.H. Weber, B. Hamann, and K.I.Joy. Construction of vector field hierarchies. In D. Ebert, M. Gross, and B. Hamann, editors, *Proc. IEEE Visualization '99*, pages 19–26, Los Alamitos, 1999.

[6] J. Helman and L. Hesselink. Representation and display of vector field topology in fluid flow data sets. *IEEE Computer*, 22(8):27–36, August 1989.

[7] Y. Lavin, R.K. Batra, and L. Hesselink. Feature comparisons of vector fields using earth mover's distance. In *Proc. IEEE Visualization '98*, pages 103–109, 1998.

[8] S.K. Lodha, J.C. Renteria, and K.M. Roskin. Topology preserving compression of 2D vector fields. In *Proc. IEEE Visualization 2000*, pages 343–350, 2000.

[9] Y. Rubner and C. Tomasi. The earth mover's distance as a metric for image retrieval. Technical report, Department of Computer Science, Stanford University, 1998. STAN-CS-TN-98-86.

[10] Y. Rubner, C. Tomasi, and L.J. Guibas. A metric for distributions with applications to image databases. In *IEEE Internations Conferences on computer Vision*, 1998.

[11] G. Scheuermann, H. Krüger, M. Menzel, and A. Rockwood. Visualizing non-linear vector field topology. *IEEE Transactions on Visualization and Computer Grapics*, 4(2):109–116, 1998.

[12] A. Telea and J.J. van Wijk. Simplified representation of vector fields. In D. Ebert, M. Gross, and B. Hamann, editors, *Proc. IEEE Visualization '99*, pages 35–42, Los Alamitos, 1999.

[13] H. Theisel. Designing 2D vector fields of arbitrary topology. *Computer Graphics Forum (Eurographics 2002)*, 21(3):595–604, 2002.

[14] H. Theisel, Ch. Rössl, and H.-P. Seidel. Compression of 2D vector fields under guaranteed topology preservation. *Computer Graphics Forum (Eurographics 2003)*, 22(3), 2003. (preprint available from http://www.mpi-sb.mpg.de/~ theisel/publications/publications.html).

[15] H. Theisel and H.-P. Seidel. Feature flow fields. In *Data Visualization 2003. Proc. VisSym 03*, 2003. (preprint available from http://www.mpi-sb.mpg.de/~ theisel/publications/publications.html).

[16] H. Theisel and T. Weinkauf. Vector field metrics based on distance measures of first order critical points. In *Journal of WSCG, Short Communication*, volume 10, pages 121–128, 2002.

[17] X. Tricoche, G. Scheuermann, and H. Hagen. A topology simplification method for 2D vector fields. In *Proc. IEEE Visualization 2000*, pages 359–366, 2000.

[18] X. Tricoche, G. Scheuermann, and H. Hagen. Continuous topology simplification of planar vector fields. In *Proc. Visualization 01*, pages 159 – 166, 2001.

[19] I. Trotts, D. Kenwright, and R. Haimes. Critical points at infinity: a missing link in vector field topology. In *Proc. NSF/DoE Lake Tahoe Workshop on Hierarchical Approximation and Geometrical Methods for Scientific Visualization*, 2000.

[20] R. Westermann, C. Johnson, and T. Ertl. Topology-preserving smoothing of vector fields. *IEEE Transactions on Visualization and Computer Graphics*, 7(3):222–229, 2001.

[21] T. Wischgoll and G. Scheuermann. Detection and visualization of closed streamlines in planar flows. *IEEE Transactions on Visualization and Computer Graphics*, 7(2):165–172, 2001.